

Hybrid metamaterial design and fabrication for terahertz resonance response enhancement

C. S. Lim¹, M. H. Hong^{1,2,*}, Z. C. Chen^{1,2}, N. R. Han², B. Luk'yanchuk¹, and T. C. Chong^{1,2}

¹Data Storage Institute, 5 Engineering Drive 1, 117608, Singapore

²Department of Electrical and Computer Engineering, 4 Engineering Drive 3, 117576, Singapore

*elemhm@nus.edu.sg

Abstract: Planar hybrid metamaterial with different split ring resonators (SRR) structure dimensions are fabricated on silicon substrates by femtosecond (fs) laser micro-lens array (MLA) lithography and lift-off process. The fabricated metamaterial structures consist of: (a) uniform metamaterial with 4 SRRs at same design and dimension as a unit cell and (b) hybrid metamaterial with 4 SRRs at same design but different dimensions as a unit cell. The electromagnetic field responses of these hybrid and single dimension metamaterial structures are characterized using a terahertz (THz) time-domain spectroscopy. Transmission spectra of these metamaterial show that a broader resonance peak is formed when 2 SRRs are close to each other. FDTD simulation proves that there is a strong mutual coupling between 2 SRRs besides a strong localized electric field at the split gap, which can enhance the electric field up to 364 times for tunable, broad band and high sensitivity THz sensing. Meanwhile, the strong coupling effect could lead to the formation of an additional resonance peak at ~0.2 THz in the THz spectra regime.

©2010 Optical Society of America

OCIS codes: (160.3918) Metamaterials; (300.6495) Spectroscopy, terahertz.

References and links

1. V. G. Veselago, "The electrodynamics of substances with simultaneously negative values of ϵ and μ ," *Sov. Phys. Usp.* **10**(4), 509–514 (1968).
2. J. B. Pendry, A. J. Holden, D. J. Robbins, and W. J. Stewart, "Magnetism from conductors and enhanced nonlinear phenomena," *IEEE Trans. Microw. Theory Tech.* **47**(11), 2075–2084 (1999).
3. J. B. Pendry, "Negative refraction makes a perfect lens," *Phys. Rev. Lett.* **85**(18), 3966–3969 (2000).
4. J. B. Pendry, D. Schurig, and D. R. Smith, "Controlling electromagnetic fields," *Science* **312**(5781), 1780–1782 (2006).
5. M. C. Wiltshire, J. B. Pendry, I. R. Young, D. J. Larkman, D. J. Gilderdale, and J. V. Hajnal, "Microstructured magnetic materials for RF flux guides in magnetic resonance imaging," *Science* **291**(5505), 849–851 (2001).
6. D. R. Smith, W. J. Padilla, D. C. Vier, S. C. Nemat-Nasser, and S. Schultz, "Composite medium with simultaneously negative permeability and permittivity," *Phys. Rev. Lett.* **84**(18), 4184–4187 (2000).
7. S. Linden, C. Enkrich, M. Wegener, J. Zhou, T. Koschny, and C. M. Soukoulis, "Magnetic response of metamaterials at 100 terahertz," *Science* **306**(5700), 1351–1353 (2004).
8. C. M. Soukoulis, S. Linden, and M. Wegener, "Physics. Negative refractive index at optical wavelengths," *Science* **315**(5808), 47–49 (2007).
9. V. M. Shalaev, W. Cai, U. K. Chettiar, H.-K. Yuan, A. K. Sarychev, V. P. Drachev, and A. V. Kildishev, "Negative index of refraction in optical metamaterials," *Opt. Lett.* **30**(24), 3356–3358 (2005).
10. B. Ferguson, and X.-C. Zhang, "Materials for terahertz science and technology," *Nat. Mater.* **1**(1), 26–33 (2002).
11. B. B. Hu, and M. C. Nuss, "Imaging with terahertz waves," *Opt. Lett.* **20**(16), 1716–1718 (1995).
12. J. Corson, R. Mallozzi, J. Orenstein, J. N. Eckstein, and I. Bozovic, "Vanishing of phase coherence in underdoped $\text{Bi}_2\text{Sr}_2\text{CaCu}_2\text{O}_{8+\delta}$," *Nature* **398**, 2211 (1999).
13. R. H. Jacobsen, D. M. Mittleman, and M. C. Nuss, "Chemical recognition of gases and gas mixtures with terahertz waves," *Opt. Lett.* **21**(24), 2011–2013 (1996).
14. N. Karpowicz, H. Zhong, C. Zhang, I. K. Lin, J. S. Hwang, J. Xu, and X. C. Zhang, "Compact continuous-wave subterahertz system for inspection applications," *Appl. Phys. Lett.* **86**(5), 054105 (2005).

15. T. J. Yen, W. J. Padilla, N. Fang, D. C. Vier, D. R. Smith, J. B. Pendry, D. N. Basov, and X. Zhang, "Terahertz magnetic response from artificial materials," *Science* **303**(5663), 1494–1496 (2004).
16. A. K. Azad, J. Dai, and W. Zhang, "Transmission properties of terahertz pulses through subwavelength double split-ring resonators," *Opt. Lett.* **31**(5), 634–636 (2006).
17. H.-T. Chen, W. J. Padilla, M. J. Cich, A. K. Azad, R. D. Averitt, and A. J. Taylor, "A metamaterial solid-state terahertz phase modulator," *Nat. Photonics* **3**(3), 148–151 (2009).
18. H. Tao, N. I. Landy, C. M. Bingham, X. Zhang, R. D. Averitt, and W. J. Padilla, "A metamaterial absorber for the terahertz regime: design, fabrication and characterization," *Opt. Express* **16**(10), 7181–7188 (2008).
19. H.-T. Chen, J. F. O'Hara, A. K. Azad, A. J. Taylor, R. D. Averitt, D. B. Shrekenhamer, and W. J. Padilla, "Experimental demonstration of frequency-agile terahertz metamaterial," *Nat. Photonics* **2**(5), 295–298 (2008).
20. C. M. Bingham, H. Tao, X. L. Liu, R. D. Averitt, X. Zhang, and W. J. Padilla, "Planar wallpaper group metamaterials for novel terahertz applications," *Opt. Express* **16**(23), 18565–18575 (2008).
21. Y. Yuan, C. Bingham, T. Tyler, S. Palit, T. H. Hand, W. J. Padilla, D. R. Smith, N. M. Jokerst, and S. A. Cummer, "Dual-band planar electric metamaterial in the terahertz regime," *Opt. Express* **16**(13), 9746–9752 (2008).
22. Y. Lin, M. H. Hong, T. C. Chong, C. S. Lim, G. X. Chen, L. S. Tan, Z. B. Wang, and L. P. Shi, "Ultrafast laser induced parallel phase change nanolithography," *Appl. Phys. Lett.* **89**(4), 041108 (2006).
23. C. S. Lim, M. H. Hong, Y. Lin, Q. Xie, B. S. Luk'yanchuk, A. Senthil Kumar, and M. Rahman, "Microlens arrays fabrication by laser interference lithography for super resolution surface nanopatterning," *Appl. Phys. Lett.* **89**(19), 191125 (2006).
24. W. J. Padilla, M. T. Aronsson, C. Highstrete, M. Lee, A. J. Taylor, and R. D. Averitt, "Electrically resonant terahertz metamaterial: Theoretical and experimental investigations," *Phys. Rev. B* **75**(4), 041102 (2007).

1. Introduction

Metamaterial are artificially engineered structures that exhibit extraordinary electromagnetic response which cannot be found in naturally available materials. The development of metamaterial is greatly stimulated by the introduction and prediction of negative refractive index or 'left-hand' materials by Veselago [1]. To realize the characteristics of a left hand meta-material, it is essential to fabricate periodic metallic resonator structure called split ring resonator (SRR) or wire cut which were first introduced by Pendry et. al. [2]. In general, SRR metamaterial are arrays of sub-wavelength scale (typically in the order of $\sim\lambda/10$) structures formed in periodical arrangement. These structures are used to manipulate the electromagnetic field in a controllable manner. Two potential applications of metamaterial are to make perfect lens [3], which is to achieve super-resolution nanofocusing beyond the diffraction limit, and cloaking effect [4], whereby light at certain wavelengths can pass through an object without any scattering thus making it 'invisible'. The benefits of metamaterial are not limited to the above mentioned applications. Research showed that the architectural SRR elements of metamaterial give one the ability to control different electromagnetic wave's electric and/or magnetic resonant response by changing the SRR designs. These phenomena of resonance tuning were demonstrated at different wavelengths, including radiowave, microwave, IR-range as well as visible light [5–9].

The development of terahertz (THz) technology, which the electromagnetic spectrum frequency lays between microwave and infra-red regions, has attracted much research attention [10]. Over the last two decades, THz radiation possesses wide applications such as THz imaging [11], spectroscopy of semiconductor and condensed matters [12], security and inspection [13,14] as well as chemical and biomedical sensing, makes it an important research subject in recent years. However, due to various challenges in detection, generation and measurement of the THz waves, intense researches have been carried out to enhance and tune the THz waves in order to close the 'THz gap'. One of important ideas is to use metamaterial with SRR scaled to the sub-THz wavelength size to obtain different THz resonance responses [15,16]. Therefore, it provides a possibility to construct novel THz devices for practical applications, such as THz modulator [17], absorber [18] and filter [19].

Conventional metamaterial with single SRR design shows single resonance peak at a certain THz frequency. With the combination of multiple SRR structures with different dimensions being fabricated together on a same substrate, multiple resonance peaks at different THz frequencies can be obtained [20,21]. Researches on the array of combination of

multiple SRR structures were carried out on the basis of each individual SRR contributing to a single resonance peak, thus results in multiple resonance frequencies. However, the effect of the mutual coupling between the adjacent SRRs is critical but not very well studied. When analyzing the electromagnetic behaviors of periodic SRR metamaterial, there is always an assumption that these structures have little effect on each other. In this paper, we design and fabricate planar hybrid metamaterial with each unit cell consisting of 4 SRRs at varied dimensions. The electric field transmission behavior of THz radiation through these hybrid metamaterial were characterized using a THz-TDS system, while the field distribution at the resonant frequencies was simulated using FDTD software.

2. Experimental setup

The SRR structures were fabricated on silicon substrates (0.4 mm thick, p-type with a resistivity of 8 - 12 Ωm) by the fs laser micro-lens array (MLA) lithography direct writing technique [22,23] and followed by lift-off process. The sample substrates were firstly coated with 1.5 μm of Microposit S1813 positive tone photoresist and baked on a hotplate for 1 min at 110°C before they were exposed by a Ti:Sapphire second harmonic generation femtosecond laser (Spectra Physics Tsunami, Mode 3960, $\lambda = 400\text{ nm}$, $\tau = 100\text{ fs}$, repetition rate = 82 MHz). A MLA was used to split and focus an incident laser beam into a series of tiny light spots. In order to control the distance between sample and MLA, the laser was coupled with a precision XY translation nanopositioning stage with computer numerical control (CNC). A high resolution precision Z stage was used to maintain a consistent gap between the MLA and samples. By moving the CNC controlled stages in X & Y directions during the laser exposure, arbitrary periodic structures can be patterned on a photoresist coated sample. The patterning was carried out by controlling the steps of the stage movement as well as the traveling speed of the stage. The development of the photoresist defines the SRR structures on the resist layer. This was followed by the deposition of 200 nm thick of Au film on the substrates by an electron beam evaporator. Acetone ultrasonic agitation was used to lift off the unwanted photoresist film and created an array of Au SRR metamaterial structures on the silicon surfaces.

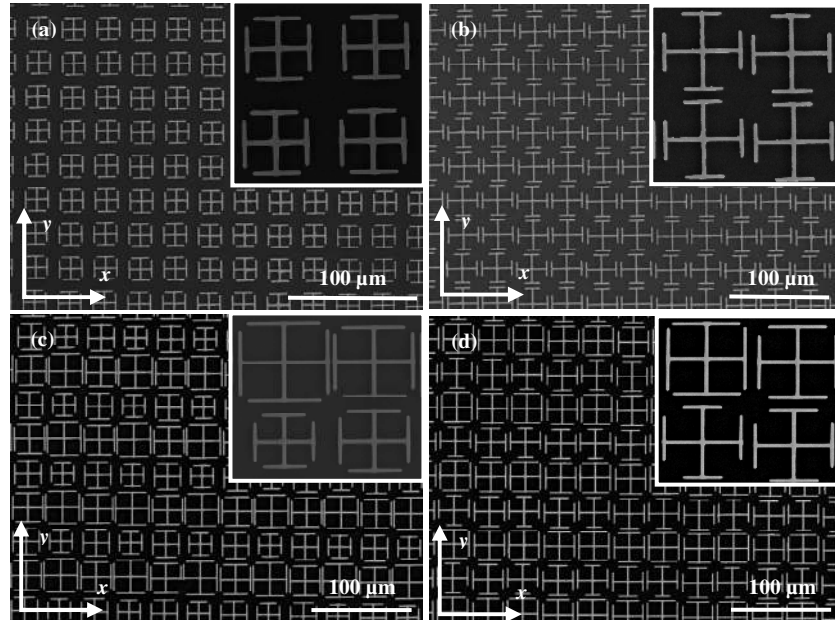
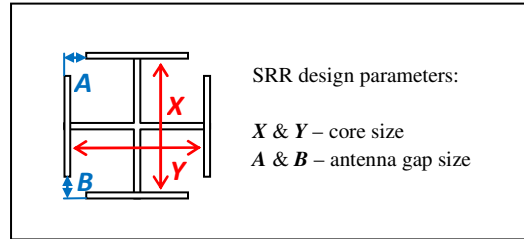
The fabricated samples were characterized with a terahertz time domain spectrometer (THz-TDS) (TPS3000, TeraView Inc.). To measure the THz transmission of the metamaterial, the samples were placed at the focused point of the THz wave at a beam diameter of $\sim 500\text{ }\mu\text{m}$. The THz wave is generated by a THz emitter that is irradiated by a femtosecond laser beam. The THz wave transmitted through the SRR meta-material structures was detected and the transmission spectra were plotted after Fourier transformation of the time-domain transmission signals. During the THz transmission spectra measurement, the THz wave propagates perpendicularly to the sample surface while its electric field and magnetic field of the THz wave are in-plane with the metamaterial structures. The polarization (electric field) is in the x direction. A THz transmission spectrum of the same bare silicon substrate was measured as a comparison reference. All the measured metamaterial spectra are normalized against the bare silicon reference spectrum. The measurement was carried out in a N_2 environment to reduce THz wave absorption by the water vapor.

3. Results and discussion

SRR metamaterial consist of an array of unit cells in which all unit cells comprise of identical SRRs. The geometry of the array and the separation between two unit cells might be different, depending on the metamaterial design. In this paper, all the designs consist of 4 SRRs as a unit cell with a unit cell separation of 75 μm . To fabricate these structures, we employed the fs laser MLA lithography technique as mentioned in the previous section. A 75 μm pitch MLA was used to generate the 4 SRRs. The MLA will direct write the first SRR on the photoresist layer, then repeat the step by stepping the MLA at x direction of 37.5 μm followed by y direction of 37.5 μm and finally x direction of $-37.5\text{ }\mu\text{m}$. Two SRR dimension

parameters are varied, one is the core size (X and Y) and the other one is the antenna gap size (A and B) as illustrated in the diagram in Fig. 1. We firstly fabricated 8 sets of samples with all the 4 SRRs as a unit cell at same design and dimensions as shown in Figs. 1(a) and 1(b). The objective to fabricate these SRR metamaterial is to study the effect of changes of SRR core size and the antenna gap size on the resonance frequency, as well as the inter-SRR interaction. The first 4 sets of the samples consist of a unit cell at the core size of 24 μm , 28 μm , 32 μm and 34 μm , respectively. The separation between 2 SRRs is maintained at 37.5 μm . When the size of the SRR increases, the separation becomes smaller and brings the 2 adjacent SRRs closer to each other. The SRR's antenna gap size was kept at 3 μm for all the individual SRR, as shown in Fig. 1(a). The other 4 sets of the samples consist of a unit cell at the antenna gap size of 2 μm , 4 μm , 6 μm and 8 μm , respectively. The separation between two adjacent SRRs is the same since the SRR core size is kept at 32 μm , as shown in Fig. 1(b).

The above-mentioned SRR metamaterial consist of only a single dimension SRRs for a unit cell and the resonance response is tuned by the SRR dimension. To study the interaction among the SRRs and obtain a broader band of resonance response, we fabricated two types of planar hybrid metamaterial structures. Each unit cell consists of 4 SRRs at same design but different dimensions. Figure 1(c) shows the Hybrid 1 metamaterial structure design. The 4 SRRs' core size inside a unit cell are 24, 28, 32 and 36 μm , as shown in Fig. 1(c). By this design, the electromagnetic field interaction between 2 SRRs can be further studied as the separation is varied. Figure 1(d) shows the Hybrid 2 metamaterial structure design. Each SRR in a unit cell has the same core size of 32 μm but the SRRs' antenna gap size are 2, 4, 6 and 8 μm within the unit cell, as shown in Fig. 1(d). By this type of hybrid structure, the electromagnetic field interaction of 2 SRRs can be tuned by the antenna gap size as the SRR separation is kept as a constant. For these 2 Hybrid designs, a strong interaction of the electromagnetic resonance coupling is observed and explained in the following section.



Metamaterial group	Size of 4 SRRs within a unit cell (μm)	
	Core size	Gap size
1	24	3
2	28	
3	32	
4	34	
5	32	2
6		4
7		6
8		8
Hybrid 1	24, 28, 32 & 34	3
Hybrid 2	32	2, 4, 6 & 8

Fig. 1. The scanning electron microscopy (SEM) images of the fabricated metamaterial structures with a unit cell consists of (a) 4 SRRs of same core size, (b) 4 SRRs of same antenna gap size, (c) Hybrid 1 design with core sizes of 24, 28, 32 and 36 μm at a constant gap of 3 μm and (d) Hybrid 2 design with gap sizes of 2, 4, 6 and 8 μm at a constant core size of 32 μm . The insert for each image shows the 4 SRR elements inside a unit cell. The lower portion of the figure gives the design geometric parameters of the metamaterials.

The transmission spectra at the THz frequencies from 0.1 to 1.5 THz for the uniform metamaterial with the unit cell at same dimension SRRs are studied. Figure 2(a) is the spectrum of the metamaterial at 4 different core sizes of 24, 28, 32 and 34 μm . For the unit cell at same SRRs core size structures, when the core size of the SRR structures decreases, there is a red shift in the THz transmission spectrum as well as a gradual decrease in the resonance peak value. The resonance frequencies of the SRR core size of 24 μm , 28 μm , 32 μm and 34 μm are 1.26, 1.06, 0.86 and 0.23 THz, respectively. According to the simplified

LC oscillator model proposed by Padilla et. al. [24], when the polarization is in plane with SRR structures while the THz propagates perpendicularly to the substrate surface, the resonance frequency of the SRR structures ω_{LC} can be described as $\omega_{LC}=(LC)^{-1/2}$. This suggests that the resonance frequency of a SRR is highly dependent on the antenna gap size of the SRR. The smaller the antenna gap size, the more red shift is the resonance frequency. As the antenna gap size of this group of SRR structures was fixed at 3 μm , the separation between 2 SRRs is the variable parameter. Therefore, the red shift is attributed to the decrease of SRRs separation which is an analogy to the reduction of antenna gap size. Meanwhile, the resonance peak becomes broader as the SRR size increases which brings the SRRs closer to each other. The full width at half maximum (FWHM) increases from 7 cm^{-1} for SRR size of 24 μm to 11.8 cm^{-1} for SRR size of 34 μm . The broadest resonance peak width for SRR size of 34 μm is due to the strong coupling effect when 2 SRRs are close to each other with only 3 μm of separation between the 2 SRRs. Another interesting phenomenon is that there is a resonance peak at a lower frequency of ~ 0.2 THz. The peak becomes stronger when the SRRs separation is closer, which attributes to the strong coupling among the SRRs within the metamaterial.

Figure 2(b) is the spectrum of the metamaterial at 4 different antenna gap sizes of 2, 4, 6 and 8 μm . When the antenna gap of the SRRs increased from 2 μm to 8 μm , a blue shift of the resonance frequency is observed. The resonances correspond to 2, 4, 6 and 8 μm gap are 0.8, 0.85, 0.95 and 1.1 THz, respectively. This can also be explained by the LC model, which is well agreed with the assumption made in this model. As the separation between 2 SRRs for all 4 sets of samples are the same, the blue shift of the resonance frequency is influenced by the antenna gap size. However, the FWHM of the peaks across the 4 gap sizes is about 7.3 cm^{-1} and vary slightly as the SRR size is kept constant at 32 μm . The curve of 2 μm antenna gap size shows another lower peak at frequency of 0.19 THz, which is quite similar to the curve of SRR size equal to 34 μm . This is due to the analogous in the structure dimension (2 μm gap versus 3 μm gap and 32 μm size versus 34 μm size). It shows that the stronger interaction among the SRRs introduces a resonance peak at this frequency.

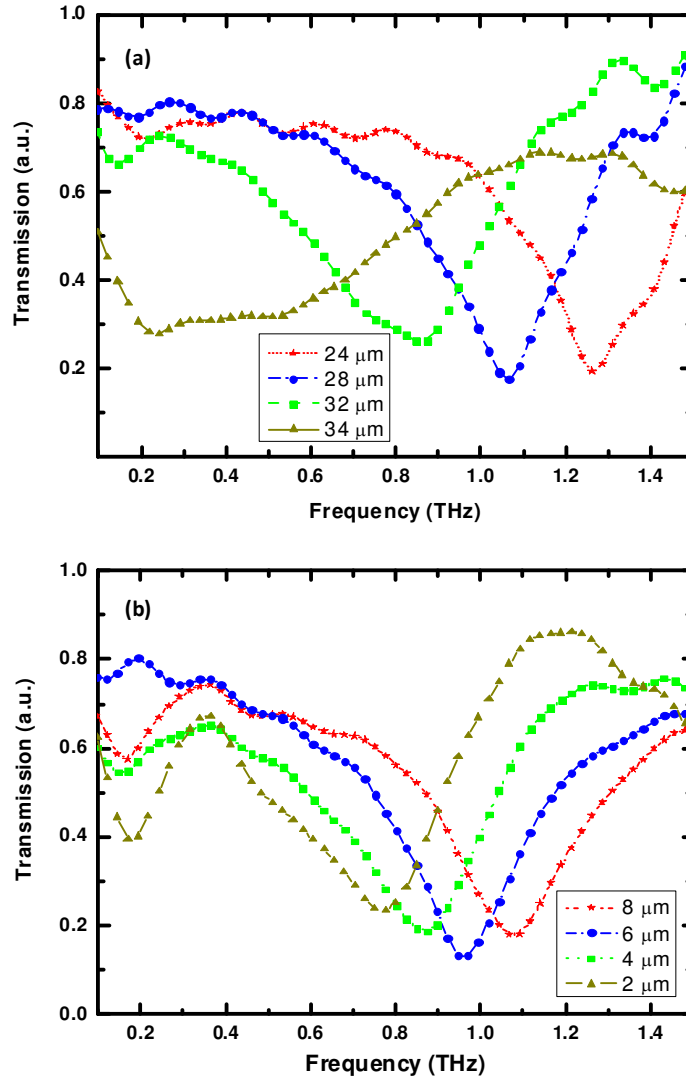


Fig. 2. The transmission spectra for the SRR metamaterial of (a) 4 SRRs with a same core size inside a unit cell (4 samples with core sizes of 24, 28, 32 and 34 μm) and (b) 4 SRRs with a same antenna gap size inside a unit cell (4 samples with gap sizes of 2, 4, 6 and 8 μm). The E-field of THz wave is along x axis.

Figure 3 shows the THz transmission spectra at 0.1 to 1.5 THz for Hybrid 1 and Hybrid 2 metamaterial structures. For the Hybrid 1 structure, 2 strong resonance peaks can be observed at 0.2 THz and 1.02 THz. Meanwhile, there were 2 weak resonance peaks at the frequencies of 1.24 and 1.45 THz, respectively. This is due to the superposition of the different resonance peaks formed by each individual core size of the SRRs as well as the mutual coupling among the SRRs. The resonance peak of the Hybrid 1 structures is weaker than the uniform core size SRR metamaterial. It is because the number of SRRs from each core size is fewer within an area of unit cell. For Hybrid 2 structures, the transmission spectra are much sharper with smaller FWHM. The Hybrid 2 SRR metamaterial structure yields a resonance at the frequency of 0.9 THz with a FWHM of $\sim 8.4 \text{ cm}^{-1}$ as shown in Fig. 3. This resonance peak is at the middle of the 4 resonance peaks formed by 4 different single SRR antenna gap size designs. There is another resonance peak at 0.225 THz similar to what we observed for

Hybrid 1 structures, which comes from the existence of electromagnetic coupling between SRRs.

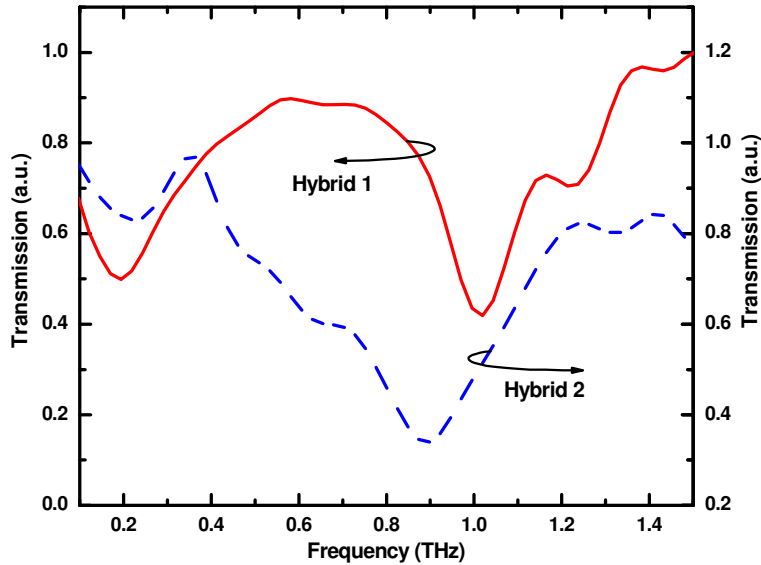


Fig. 3. The measured THz-TDS transmission spectra for the Hybrid 1 design with SRR core size varied and the Hybrid 2 design with SRR antenna gap size varied. The plots are normalized against the measured transmission spectra of the bare silicon substrate.

In order to understand the effect of the mutual coupling of the SRRs in metamaterial, we carried out theoretical simulation using CST Finite difference time-domain software to investigate the field distribution of the hybrid structures. Figure 4 shows the E-field distribution of (a) Hybrid 1 and (b) Hybrid 2 designs, respectively. It can be observed that Hybrid 1 design gives the THz E-field enhancement of ~ 190 times, while Hybrid 2 design has an E-field enhancement of ~ 364 times. For the Hybrid 1 design, the localized enhancement is particularly strong around the separation region between the 2 SRRs with core sizes of $36 \mu\text{m}$ and $32 \mu\text{m}$. The strong E-field interaction between these 2 SRRs is observed due to the closer separation distance. For the other 2 SRR core sizes (24 and $28 \mu\text{m}$), the enhancement is concentrated at the antenna gap with little interaction at the separation region. This is because the reduction in the SRR core size increases the SRRs separation, thus leads to less coupling effect. This is a new phenomena observed from this design. For the Hybrid 2 design, the enhancement is higher than that for the Hybrid 1 design. It is because there is higher density of SRRs close to each other. The higher density of SRRs gives more coupling between the SRRs as all the SRRs are only $5.5 \mu\text{m}$ apart from one to another. This implies that the mutual coupling of the SRRs plays an important role in determining the resonance peak as well as the magnitude of the E-field enhancement. The experimental and simulation results show that the hybrid SRR metamaterial designs can provide a high THz detection sensitivity and flexibility in tuning THz resonance response to enhance THz sensing and detection.

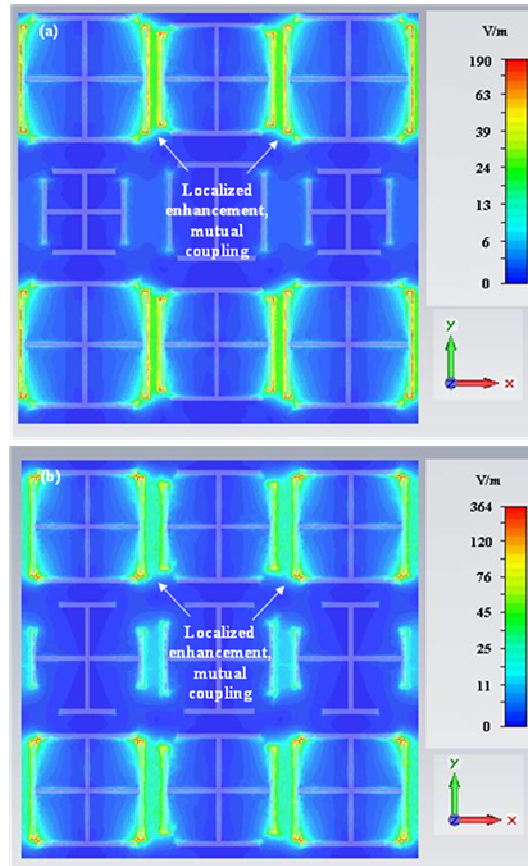


Fig. 4. FDTD simulation results of the electric field distribution on the SRR metamaterial structures for (a) Hybrid 1 and (b) Hybrid 2 designs. The direction of the electric field vector of the THz wave is in the x direction.

4. Conclusions

In summary, planar uniform and hybrid SRR metamaterial were designed and successfully fabricated by femtosecond laser MLA lithography. The SRR meta-material structures were characterized by THz-TDS technique to measure their THz transmission spectra. It is found that interaction among the SRRs in metamaterial creates a strong mutual coupling within the region between 2 SRRs. The transmission spectra show a broad band resonance peaks. It is no longer a simple combination of distinctive individual resonance peak from each SRR size. It becomes broader as the SRRs are brought closer to each other. The coupling effect also introduces an additional peak at the lower frequency of THz regime at ~ 0.2 THz. The FDTD simulation of the hybrid SRR metamaterial structures at resonance frequencies confirms the strong coupling among the SRRs within the meta-materials. The hybrid SRR metamaterial designed and fabricated provide a novel approach to realize tunable and broad band THz response for the THz detection sensitivity enhancement.

Acknowledgements

The authors would like to acknowledge the funding provided by ASTAR SERC Terahertz Program (Project No. 082 141 0039) for the research work published in this paper.